Kidney International, Vol. 67 (2005), pp. 931–943

Activation of ERK in renal fibrosis after unilateral ureteral obstruction: Modulation by antioxidants

BETTY PAT, TAO YANG, CHUIZE KONG, DIANNE WATTERS, DAVID W. JOHNSON, and GLENDA GOBE

Department of Molecular and Cellular Pathology, School of Medicine, University of Queensland, Herston, Australia; Department of Urology, China Medical University, Shenyang, People's Republic of China; School of Biomedical and Biomolecular Sciences, Griffith University, Nathan, Australia; and Department of Renal Medicine, Princess Alexandra Hospital, Ipswich Road, Woolloongabba, Brisbane, Australia

Activation of ERK in renal fibrosis after unilateral ureteral obstruction: Modulation by anti-oxidants.

Background. A recent in vitro model of oxidative stress-induced renal fibrosis demonstrated that activated or phosphorylated extracellular signal-regulated protein kinase (pERK) played a role in apoptosis of renal fibroblasts, but not tubular epithelium where it promoted cell growth and survival. The present study utilized an in vivo model of renal fibrosis after unilateral ureteral obstruction (UUO) to examine the relationship between pERK, apoptosis, proliferation, and differentiation in renal fibroblast and tubular epithelial cells, in comparison with the in vitro results.

Methods. UUO was induced in rats for 0 (controls, untreated), 6, and 24 hours, 2, 4, and 7 days ($N = 4$), and tissue analyzed for fibrotic characteristics using microscopy and special stains, Western immunoblots and reverse transcription-polymerase chain reaction (RT-PCR). Controls and UUO animals were also treated with vitamin E, N-acetylcysteine (NAC), or fluvastatin to assess any antioxidant effect on attenuation of fibrosis and pERK expression.

Results. Azan stain and α-smooth muscle actin (α-SMA), collagen III, and fibronectin expression confirmed development of UUO-induced fibrosis. Oxidative stress markers heme oxygenase-1 (HO-1) and 8-hydroxy-2′-deoxyguanosine (8-OHdG) confirmed oxidative stress at all UUO time points. Tubular epithelial and interstitial mitosis and apoptosis were significantly increased over controls at 2 to 7 days after UUO ($P < 0.01$). The pERK/ERK ratio increased significantly at 1 to 7 days of UUO in comparison with controls (three- to fivefold, $P < 0.05$). There was a significant spatiotemporal correlation between pERK and tubular epithelial proliferation ($P < 0.001$). pERK occasionally colocalized with apoptotic cells (dual labeling) in the interstitium but not in the tubular epithelium. Fluvastatin was the only treatment that attenuated fibrosis (decreased α-SMA, fibronectin, tubular epithelial apoptosis) and it also significantly decreased expression of 8-OHdG at 2 and 7 days ($P < 0.05$). It was associated with decreased pERK at 7 days, compared with UUO alone ($P < 0.05$).

Conclusion. Promotion of tubular epithelial proliferation and survival, and interstitial cell apoptosis, may minimize renal fibrosis after UUO. In the present study, both were linked spatially and temporally with increased pERK expression. Fluvastatin treatment attenuated UUO-induced fibrosis via an antioxidant and pERK-related mechanism.

Key words: apoptosis, oxidative stress, ERK, renal fibrosis, signal transduction pathways.

Received for publication July 10, 2003
and in revised form December 1, 2003, and August 13, 2004
Accepted for publication September 28, 2004

Ureteral obstruction leads to tubulointerstitial fibrosis, a process that involves increasing populations of interstitial inflammatory cells, such as myofibroblasts [1], lymphocytes and macrophages [2], activation and transdifferentiation of intrinsic renal cells [3], and increasing tubular atrophy and interstitial extracellular matrix (ECM) accumulation [4, 5]. Tubular atrophy is associated with increased apoptosis that is not balanced by elevated levels of tubular cell proliferation seen in the early or acute stages of renal fibrosis [6–8]. Although considerable advances have been made in understanding the pathogenesis of renal fibrosis due to unilateral ureteral obstruction (UUO), there are few published data, either experimental or clinical, that describe the early transduction events of fibrogenic signals. These pathways need further definition.

Although the pathogenesis of tubulointerstitial fibrosis is undoubtedly multifactorial, one of its early modulators is oxidative stress [9–12]. Localized oxidative stress may be cytotoxic to renal tubular epithelial cells [13, 14], resulting in increased apoptosis [15]. There is also some indication that oxidative stress plays a role in transforming growth factor-β1 (TGF-β1) expression and in production of ECM in tubulointerstitial fibrosis [16]. Attenuation of renal fibrosis may occur via a fluvastatin-induced reduction of oxidative stress [12]. Oxidative stress has been linked to tubulointerstitial fibrosis via the activation of intracellular second messenger signaling pathways, for example, after diabetic nephropathy (reviewed in [17]). More specifically, members of the mitogen-activated protein kinase (MAPK) family of signaling molecules, one of the best-characterized of the signal transduction families,

are known to be activated in renal cells by oxidative stress [18, 19].

The MAPK family utilizes three parallel signaling pathways: extracellular signal-regulated kinase (ERK); stress-activated protein kinase/c-Jun amino terminal kinase (SAPK/JNK); and p38 MAPK [20]. The ERK pathway is usually stimulated by serum and growth factors and activation of its cascade stimulates mitosis, cell differentiation, and in some cells, hypertrophy [21]. ERK activation has been identified in proliferative glomerulonephritis in rats [22] and it may play a role in oxidant-dependent pathways that lead to renal injury [23]. Additionally, there are emerging data indicating that hydrogen peroxide (H_2O_2) can activate ERK in association with cell death [19, 24–26]. This association may be specific to different cell types making up the renal population. For example, in an in vitro model of oxidative stress-induced renal fibrosis, activated or phosphorylated ERK (pERK) was part of the apoptotic pathway of renal fibroblasts, in comparison to the renal tubular epithelium where it supported cell survival [19].

The present study utilized an in vivo model of renal fibrosis after UUO in rats to examine the relationship between pERK, apoptosis, proliferation, and differentiation in renal fibroblast and tubular epithelial cells. The aim of this study was to characterize the changes in pERK expression and localization over a 7-day period after UUO in comparison with oxidative stress [measured by oxidative stress markers heme oxygenase-1 (HO-1) or 8-hydroxy-2′-deoxyguanosine (8-OHdG) [27]], and known characteristics of tubulointerstitial fibrosis [α-smooth muscle actin (α-SMA), collagen, fibronectin], cellular proliferation [proliferating cell nuclear antigen (PCNA)], and apoptosis [morphology and in situ end labeling (ISEL)]. Colocalization between pERK and PCNA, α-SMA or ISEL was examined. The results were compared with those found using an in vitro oxidative stress model of renal fibrosis [19]. The effects of cotreatment of UUO-associated fibrosis with the putative antioxidants vitamin E, N-acetylcysteine (NAC), or fluvastatin were also investigated.

METHODS

Animals and surgery

All experiments were performed with ethics approval from the University of Queensland Animal Experimentation Ethics Committee (Number Path/RBH/732/03/RD). Male Sprague-Dawley rats weighing 180 to 220g were allowed free access to water and standard rat food and were housed in an air-conditioned room with 12/12 hours light/dark cycle. Animals were anesthetized with pentobarbital sodium (60 mg/kg, intraperitoneally). Normal body temperature was maintained throughout surgery. Animals were divided into sets of controls (no operation) and UUO animals, which were or were not treated with the antioxidants vitamin E (40 mg/kg/day), NAC (50 mg/kg/day) (both Sigma-Aldrich, Sydney, Australia), or fluvastatin (40 mg/kg/day) (Novartis Pharmaceuticals Australia Pty. Ltd., North Ryde, Australia) ($N = 4$ per control or treatment group). UUO or control sets were studied for 6 and 24 hours and 2, 4, or 7 days. Sham surgery was not used for controls based on previous work [6] indicating no difference between untreated and sham-operated controls. For UUO groups, the left kidney was exposed with a midabdominal incision and a double ligature placed on the left ureter approximately 1 cm from the renal hilum, before closing the abdominal incision with 4-0 silk and Michel clips. The antioxidants were either either injected intraperitoneally (vitamin E and NAC) or were administered by oral gavage (fluvastatin in 1% methyl cellulose). Control groups for antioxidant treatments received an injection or gavage vehicle. For tissue collection, animals were heavily anesthetized, aortic blood was collected for function studies, and then both kidneys removed prior to the animal's death.

Preparation of tissue

Each kidney was quickly sliced transversely (2 to 3 mm slices) to the length of the kidney. The slices closest to the equatorial plane were either fixed in 10% buffered formalin for histology and immunohistochemistry, or snap frozen in liquid nitrogen and stored at −80°C in 22-oxacalcitriol (OCT) for frozen sections, if required. The adjacent slices were frozen at −80°C in two lots for either protein or RNA extraction and analysis. Note: Several human UUO samples ($N = 4$) were available from the Department of Nephrology, China Medical University, Shenyang, People's Republic of China (Professor C. Kong) and they were sectioned and used for comparison with rat samples, using hematoxylin and eosin staining and immunohistochemistry.

Histology

Formalin-fixed tissue was embedded in paraffin using routine methods, 4 μm sections were cut onto Superfrost Plus histology slides, and stained with hematoxylin and eosin (routine histology), Azan stain for collagen and fibrosis, ISEL for apoptosis, PCNA for cell proliferation, periodic acid-Schiff (PAS) reagent for identification of proteinaceous casts, α-SMA for identification of myofibroblasts, and pERK for localization of the activated ERK protein.

Immunohistochemistry or immunofluorescence

Subserial sections were cut, numbered, deparaffinized, and rehydrated, before staining with the peroxidase-antiperoxidase method. Nonspecific binding of peroxidase or antibodies was blocked with 0.3% H_2O_2 in 4%

skim milk powder (blotto) followed by incubation in diluted normal rabbit or goat serum. Primary antibodies were α-SMA (mouse monoclonal) (Sigma-Aldrich Pty Ltd, Sydney, Australia) (1:100 dilution), PCNA (mouse monoclonal) (Dako, Glostrup, Denmark) (1:50 dilution), pERK (rabbit polyclonal) (New England Biolabs, Beverly, MA, USA) (1:400 dilution), and 8-OHdG (goat polyclonal) (Chemicon, Boronia, Australia) (1:2000 dilution) used as a marker of oxidative stress in situ [27]. The appropriate secondary antibody was applied at a dilution of 1:200 to 1:400 in Tris buffer. Secondary antibodies were either conjugated to Alexa-Fluor or Texas Red fluorophores for immunofluorescence (Molecular Probes, Eugene, OR, USA) or the peroxidase-antiperoxidase reaction plus the chromogen diaminobenzidine tetrahydrochloride (DAB) for immunohistochemistry. Negative controls were prepared without primary antibody, or with nonspecific serum. Positive tissue control sections from unrelated studies were included. Sections were lightly counterstained with hematoxylin and then dehydrated in ethanols, cleared in xylene and mounted in Depex.

Double staining using immunofluorescence. In some instances, double staining for proteins was used in paraffin sections. Rehydrated sections were washed in Tris-buffered saline (TBS)/0.1% Tween-20 (TBST) and nonspecific sites were blocked with 3% bovine serum albumin (BSA) in TBST for 1 hour at room temperature. Sections were incubated with primary antibody against pERK (1:400) in 3% BSA in TBST overnight at 4°C. Sections had 3 × 10 minute washes in TBST, then incubation with a second primary antibody (from a different species to the first primary antibody) against α-SMA (1:50) in 1% BSA in TBST for 1 hour at room temperature in the dark. Sections were washed 3 × 30 minutes in TBST, then incubated with a fluorescent secondary antibody mixture containing an Alexa-Fluor labeled goat α-rabbit IgG and Texas Red-X–labeled goat α-mouse IgG (Molecular Probes), each at a dilution of 1:200 in 1% BSA in TBST for 1 hour at room temperature. Sections were washed 3 × 30 minutes in TBS, then mounted with glass coverslips using either Dako fluorescent antifade mounting medium (Dako, Botany, New South Wales, Australia) or Vectashield mounting medium for fluorescence with 4′-6-diamadino-2-phenylindole (DAPI) (Vector Laboratories, Burlingame, CA, USA) and allowed to set overnight in the dark prior to fluorescence microscopy.

ISEL

Following published methods [28, 29], sections were dewaxed, rehydrated, digested in 0.5% pepsin in 0.1 mol/L HCl for 15 minutes at 37°C, then washed in TBS. Cells with DNA strand breaks were detected using a reaction mix containing Klenow DNA polymerase I and biotin-labeled deoxyuridine triphosphate (dUTP), as well as other products necessary for the ISEL reaction mix [29] (all products from Roche Diagnostics, Castle Hill, Australia). Endogenous peroxidase activity was blocked with 0.1% H_2O_2, and biotin-labeled nuclei visualized with horseradish peroxidase-conjugated avidin (Dako) developed in DAB and counterstained with hematoxylin. Negative controls had no Klenow polymerase, and positive controls were rat renal sections from other experiments in which high levels of ISEL were known to correlate with high levels of apoptosis assessed morphologically. Alternatively, sections were stained using a similar end-labeling procedure using a commercially available ApopTag® Peroxidase In Situ Apoptosis Detection Kit according to the manufacturer's protocol for paraffin-embedded sections (Serologicals Corporation, Chemicon). For dual labeling of apoptosis and pERK, the ApopTag® Kit was used first and methods completed to DAB and a buffer wash, then routine pERK immunofluorescence methods were applied and sections mounted in antifade aqueous mounting medium.

Assessment of morphologic and immunohistochemistry characteristics

As far as possible, assessments were carried out with no knowledge of treatment, although the dilatation of the renal pelvis with progressive UUO made some time points obvious during microscopy. Light microscopic evaluation was performed using a magnification of ×400 in 10 to 20 randomly selected fields and recorded, where appropriate, as positive cells per mm^2 of tissue (the field of view at ×400 was 0.0625 mm^2 for the microscope used for all analyses). Results are presented as mean ± standard error of the mean (SEM). Control sections had no pathologic changes.

Azan-stained sections. Blue collagen staining of the tubulointerstitium in Azan-stained sections was scored (Azan score) as the% range of tubules showing thickening of the basement membrane and expansion of the surrounding interstitium (for example, 0% collagen stain, 0; 1% to 25%, 1; 26% to 50%, 2; and >50%, 3). Staining of normal basement membrane and vessel walls was ignored.

Apoptosis. Previously defined morphologic criteria were used to count apoptotic cells in the tubular epithelium or interstitium of hematoxylin and eosin–stained sections [30]. These characteristics included cellular rounding and shrinkage, eosinophilic cytoplasm, nuclear chromatin compaction, especially along the nuclear envelope in a crescentic manner, membrane-bound cellular blebbing, and formation of apoptotic bodies which may appear in the tubular lumina or be phagocytosed by intrinsic renal cells or invading macrophages.

ISEL. ISEL nuclear positivity was counted in epithelial and interstitial cells. ISEL is an indication of DNA fragmentation and equates well with apoptosis when morphologic comparisons are made. For example, a comparison between apoptosis assessed using morphology versus

ISEL produced a Pearson's $R = 0.6833$ with significance at $P < 0.0001$ in a two-tailed test.

Cell proliferation. PCNA-positive nuclei were counted. Mitotic nuclei were also assessed in comparison with PCNA labeling.

α-SMA and pERK immunohistochemistry. Immunolocalization in the tubulointerstitium was recorded. α-SMA positivity of vessel walls was ignored. Where double labeling of pERK and PCNA (pERK/PCNA) was used, counts were calculated as a % of all labeled cells for pERK or PCNA alone or dual-labeled cells and presented as a graph of pERK/PCNA against pERK labeling for each time point.

8-OHdG immunohistochemistry. Localization and expression intensity of 8-OHdG in the tubulointerstitium were recorded at ×400 magnification in batch-stained sections using a range where 0 was no labeling, 1 was <50% area labeling of low intensity; 2 was <50% area labeling with high intensity; 3 was >50% area labeling with low intensity; and 4 was >50% area labeling of high intensity. Means ± SEM were calculated for each experimental group and recorded as an index of expression.

Western blot for protein analysis

Tissue was disrupted in ice-cold cell lysis buffer (50 mmol/L Tris-Cl, pH 7.5, 150 mmol/L NaCl, 1% Nonidet P-40, 0.1% sodium dodecyl sulfate (SDS), 25 mmol/L sodium fluoride, and 0.5 mol/L ethylenediaminetetraacetic acid) containing protease and phosphatase inhibitors (100 μg/mL phenylmethylsulfonyl chloride, 20 μg/mL leupeptin, 20 μg/mL aprotinin, and 1 mmol/L sodium orthovanadate) (all Sigma-Aldrich products) using a tissue homogenizer. Cell debris was removed by centrifugation at 16,000*g* for 15 minutes at 4°C. Protein concentration was determined in each tissue extract by a Bradford protein assay (Bio-Rad Pty Ltd., Sydney, New South Wales, Australia) and spectroscopy at 595 nm. Between 20 and 40 μg of total protein were electrophoresed on a 8% to 12% SDS-polyacrylamide gel using a Bio-Rad mini-protean unit, transferred to a polyvinylidene difluoride (PVDF) membrane, and blotted routinely with ERK (1:1000), pERK (1:1000), HO-1 (Stressgen, Victoria, British Columbia, Canada) (1:2000), α-SMA (1:2000), collagen III (Research Diagnostics Inc., Flanders, NJ, USA) (1:1000), and fibronectin (BD Biosciences Pharmingen, North Ryde, New South Wales, Australia) (1:1000) primary antibodies, then appropriate horseradish peroxidase-conjugated secondary antibodies diluted (1:2000) in 5% blotto. Immunoblotting with anti-HO-1 antibody was used as an indirect measurement of oxidative stress, along with reverse transcription-polymerase chain reaction (RT-PCR) (details below). HO-1 is an inducible form of the HO enzyme [31], which has been shown to be a reliable and early marker of oxidative stress in renal disease [32–34]. Protein bands were visualized using enhanced chemiluminescence (ECL). X-ray film was scanned using a Hewlett Packard ScanJet 3200C at 300dpi and Scion Image (β4.0.2) software was used to quantify the density of the bands in arbitrary densitometry units. Membranes were routinely stained with Coomassie Blue (Sigma-Aldrich), or actin immunoblots were used, to verify equal protein loading of lanes. Positive cell extracts from antibody suppliers were routinely used as positive controls for immunoblots.

RT-PCR of HO-1

Total RNA was extracted using Qiagen's RNeasy Mini Prep Kit (Qiagen, Sydney, New South Wales, Australia) according to the manufacturer's protocols for animal tissue. Total RNA was eluted with RNase-free H_2O in a final volume of 50 to 60 μL. Extracted RNA was tested for purity and integrity by spectrophotometry at 260 nm and 280 nm and electrophoresed on a 1.5% formaldehyde agarose gel prior to RT-PCR. RNA was routinely treated with DNA-free™ (Ambion, Austin, TX, USA) to remove contaminating genomic DNA. One to three micrograms were reverse transcribed in a total reaction volume of 20 μL using the Superscript™ First Strand Synthesis System for RT-PCR (Invitrogen, Life Technologies, Sydney, New South Wales, Australia). Controls lacking Superscript™ enzyme (no RT) or template RNA (−R) and control RNA (provided by the manufacturer) were run in conjunction with all sample reactions to monitor the efficiency and integrity of the RT reaction. Primers for rat HO-1 were designed in Primer 3.0 software (MIT) from rat HO-1 cDNA sequence (NCBI Genbank database accession number NM 012580) [35]. The HO-1 primer pair used for PCR was forward primer (5′-CAGTCTATGCCCCGCTCTAC-3′) and reverse primer (5′-ACCAGCAGCTCAGGATGAGT-3′). β-actin was utilized as a loading control using the following forward primer (5′-ACTATCGGCAATGAGCGGTTC-3′) and reverse primer (5′-ATGCCACAGGATTCCATACCC-3′).

Renal functional parameters

Plasma sodium, potassium, creatinine, blood urea nitrogen (BUN), and lactate dehydrogenase (LDH) were measured using a Hitachi Modular Blood Analyzer (Hitachi Australia, Milton, Australia) at the Queensland Health Pathology and Scientific Services Unit, Royal Brisbane Hospital, Brisbane, Australia.

Statistical analyses

Data were analyzed using standard statistical methods, linear regression, Student *t* test, one-way analysis of variance (ANOVA) and Dunnet's multiple comparison or

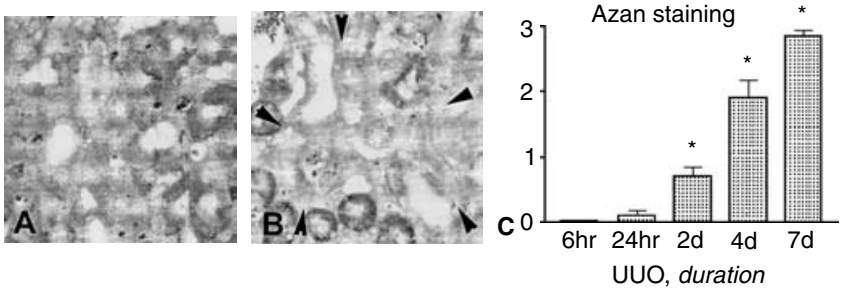

Fig. 1. Azan staining for collagen. Histochemistry for 4 (*A*) and 7 (*B*) days' unilateral ureteral obstruction (UUO) animals shows an increasing amount of tubulointerstitial collagen (blue stain), with a large area of fibrosis marked with arrowheads (B). The Azan scores (mean ± SEM of the degree of collagen) are presented graphically (*C*) and demonstrate a significant increase in Azan scores at 2 to 7 days UUO. $^*P < 0.05$.

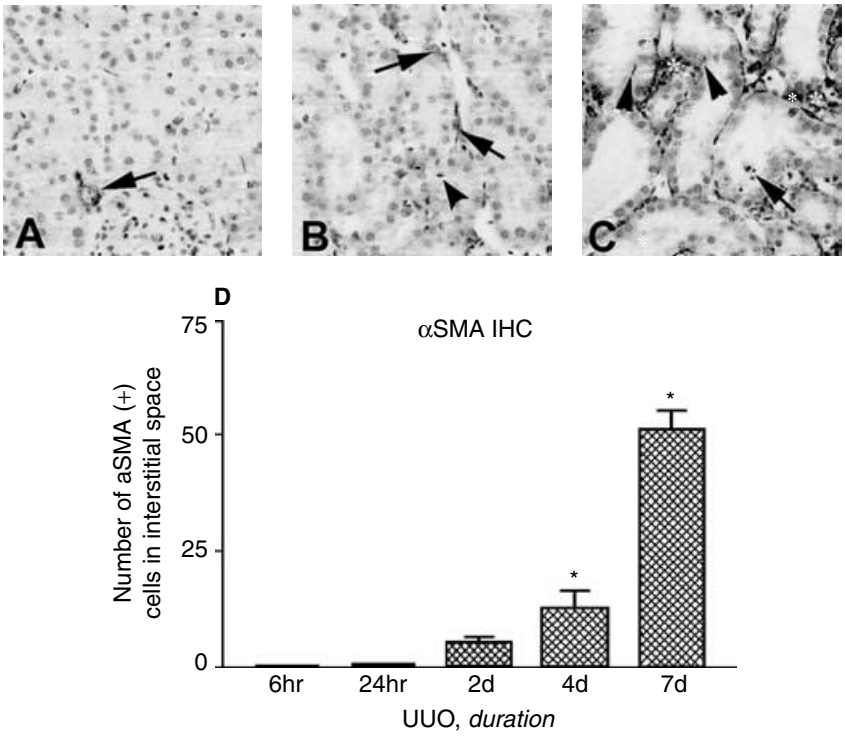

Fig. 2. α-Smooth muscle actin (α-SMA) immunohistochemistry (IHC). (*A*) Control staining is demonstrated, where only vessels stained positive (arrow). (*B* and *C*) α-SMA positivity in the interstitium of 2 and 7 days' unilateral ureteral obstruction (UUO) animals (white asterisks) (arrowheads and an arrow indicate mitotic and apoptotic cells, respectively). (*D*) Mean ± SEM of α-SMA–positive cells per mm^2 of tissue in UUO animals. There was a significant increase in interstitial cell positivity at 4 and 7 days' UUO. $^*P < 0.05$.

Bonferroni's post test using Graphpad Prism (version 3.0) and Stata (version 8.0) statistical software. Most data are presented in graphic form as the mean ± SEM. Significance was assessed at $P < 0.05$.

RESULTS

Renal function

There were no significant differences found in any of the selected functional parameters of UUO animals in comparison with controls in the 7 days studied. Compensatory functional changes in the right non-UUO kidney were thought to maintain normal bilateral renal function as measured by plasma chemistry [36].

Development of fibrosis in UUO groups

Fibrosis was assessed by Azan histochemical staining for collagen, α-SMA immunostaining for activated fibroblasts, and whole tissue protein expression by Western immunoblot analysis for α-SMA, collagen III, and fibronectin. Figure 1A and B demonstrate Azan staining in 4 and 7 day UUO animals and Figure 1C represents the mean ± SEM of the Azan score. There was a significant increase in Azan score at 2, 4, and 7 days UUO in comparison with 6 and 24 hours' UUO animals ($P < 0.05$). Immunohistochemistry of α-SMA is presented in Figures 2A to C. Figure 2A shows labeling of α-SMA only in vessels of control kidneys. α-SMA–labeled cells increased in the interstitium over time in UUO animals (Fig. 2B and C) (2 and 7 days, respectively). The mean number of α-SMA–positive interstitial cells increased significantly in 4 and 7 days' UUO kidneys in comparison with controls ($P < 0.05$) (Fig. 2D). There were no α-SMA–positive cells in the tubular epithelium. Figure 3 demonstrates representative Western blots for whole kidney protein expression of α-SMA, collagen III, and fibronectin for control or UUO animals. All fibrotic markers were significantly increased in UUO animals at 4 or 7 days ($P < 0.05$) in

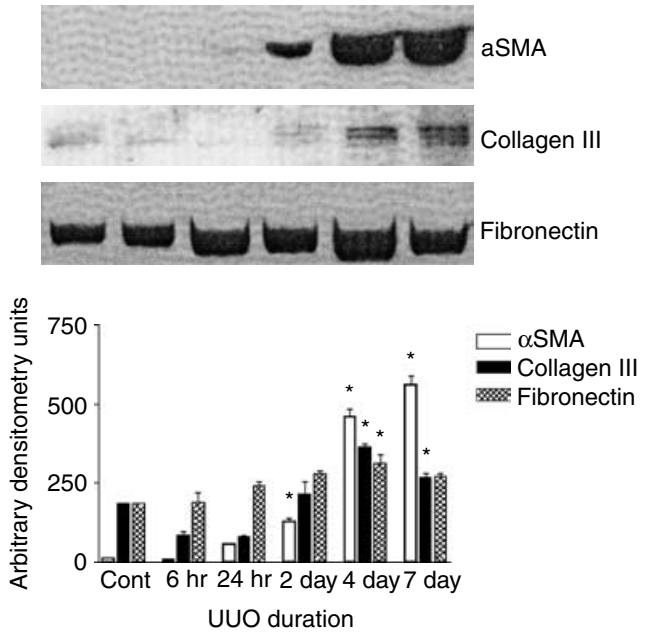

Fig. 3. Markers of fibrosis. Western blots for α-smooth muscle actin (α-SMA), collagen III, and fibronectin (selected fibrotic markers) and the associated densitometry (mean ± SEM) are presented for control or unilateral ureteral obstruction (UUO) animals. There was a significant increase in expression of all fibrotic markers at 4 and 7 days' UUO. $^*P < 0.05$ in comparison with controls.

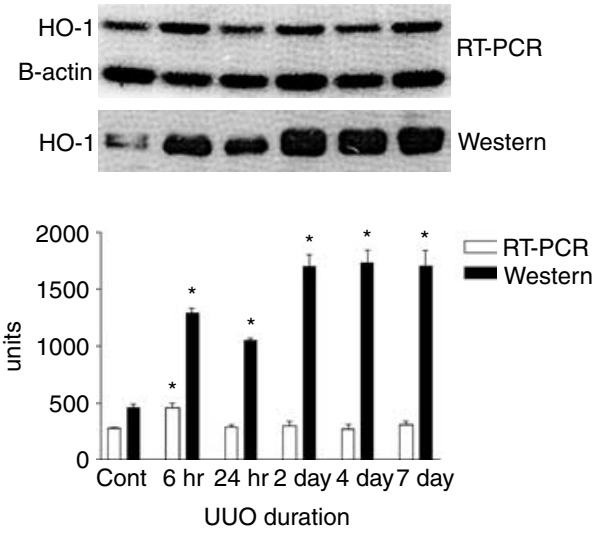

Fig. 4. Heme-oxygenase (HO-1) expression. Reverse transcription-polymerase chain reaction (RT-PCR) indicates a significant peak in HO-1 transcription ($P < 0.01$) at 6 hours' unilateral ureteral obstruction (UUO) after β-actin normalization and Western immunoblot and densitometry demonstrate a significant and increasing level of HO-1 protein in total kidney from 6 hours to 7 days' UUO. $^*P < 0.01$.

comparison with controls, confirming the development of significant fibrosis by these times.

UUO induction of oxidative stress

The involvement of oxidative stress in the development of UUO-induced fibrosis was assessed by HO-1 induction (Fig. 4). RT-PCR indicated a significant peak in HO-1 transcription (normalized to β-actin) at 6 hours UUO ($P < 0.01$). Western blot analysis and densitometry demonstrated a significant and increasing level of HO-1 protein in total kidney from 6 hours to 7 days UUO ($P < 0.01$). The 8-OHdG immunohistochemistry index verified the induction of oxidative stress in UUO kidneys (data presented in following section on modulation of fibrosis).

Tubulointerstitial mitosis and apoptosis

Mitosis and apoptosis in the tubular epithelium and in the interstitium were compared and results are presented as histology and quantification. Labeling of PCNA-positive nuclei in 2 and 7 days' UUO kidneys was consistently and significantly higher than controls (Fig. 5A to C). Using both morphology (Fig. 5D) and PCNA (Fig. 5E) for quantification, mitosis peaked in the tubular epithelium at 2 days' UUO and remained significantly elevated at 4 and 7 days ($P < 0.01$ to $P < 0.05$). In the interstitium, a moderate but significant increase in interstitial cell proliferation occurred from 2 to 7 days' UUO, indicating an increase in interstitial inflammatory cell populations. Figure 6A and B demonstrates apoptosis in the tubular epithelium and interstitium in hematoxylin and eosin sections, and Figure 6C demonstrates ISEL verification of apoptosis. The levels of tubular epithelial apoptosis were significantly greater than controls at 2, 4, and 7 days' UUO, peaking at 7 days' UUO (Fig. 6D) [2 and 4 days' UUO ($P < 0.05$) and 7 days' UUO ($P < 0.001$, compared with controls)]. Interstitial apoptosis occurred at moderate levels and was significantly greater than controls at 2 and 4 days' UUO ($P < 0.05$). The increased levels of apoptosis in the interstitium may indicate an attempt by the UUO kidneys to control an increasing and abnormal interstitial population in the early stages of fibrosis [37]. The absolute numbers of mitotic versus apoptotic cells per mm^2 of tissue in the tubular epithelium (Figs. 5D and 6D) indicated increasing apoptosis and decreasing mitosis at 7 days. These results explain, in part, the development of tubular atrophy that is integral to the pathogenesis of tubulointerstitial fibrosis after UUO.

ERK activation and localization after UUO

In an in vitro model of renal fibrosis induced by oxidative stress, pERK played a part in sustaining survival of renal tubular epithelial cells versus cell death of renal fibroblasts [19]. In the present investigation, expression of pERK was analyzed during development of UUO-induced renal fibrosis and pERK localization was compared with localization and levels of cell proliferation, death, and differentiation in the tubular epithelium versus interstitium. Western blotting or immunohistochemistry verified the presence of pERK, minimally in controls

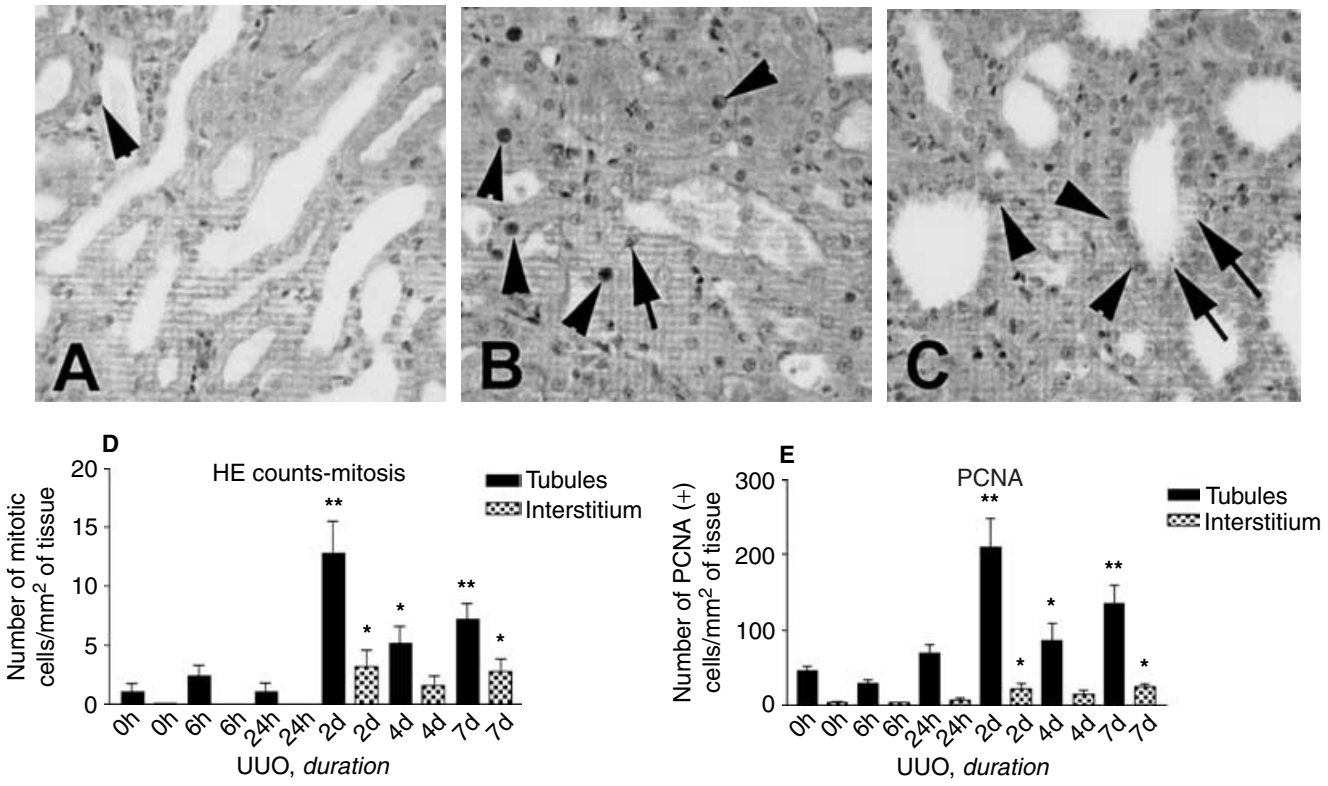

Fig. 5. Mitosis in the tubulointerstitium. (*A* to *C*) Proliferating cell nuclear antigen (PCNA) immunohistochemistry (IHC) in control, 2 and 7 days' unilateral ureteral obstruction (UUO) animals, respectively. Examples of PCNA-positive nuclei are demonstrated with arrowheads. (B) A mitotic cell (morphology) is indicated with an arrow. (*C*) Apoptotic bodies can be seen in the tubular epithelium (arrows) as well as PCNA-positive nuclei (arrowheads). (*D*) The mitotic counts per mm^2 of tissue using morphology. (*E*) Counts of PCNA-positive nuclei. In each case, there were significant increases in epithelial and interstitial cell proliferation at 2 to 7 days' UUO. $^{**}P < 0.01$; $^{*}P < 0.05$ in comparison with controls.

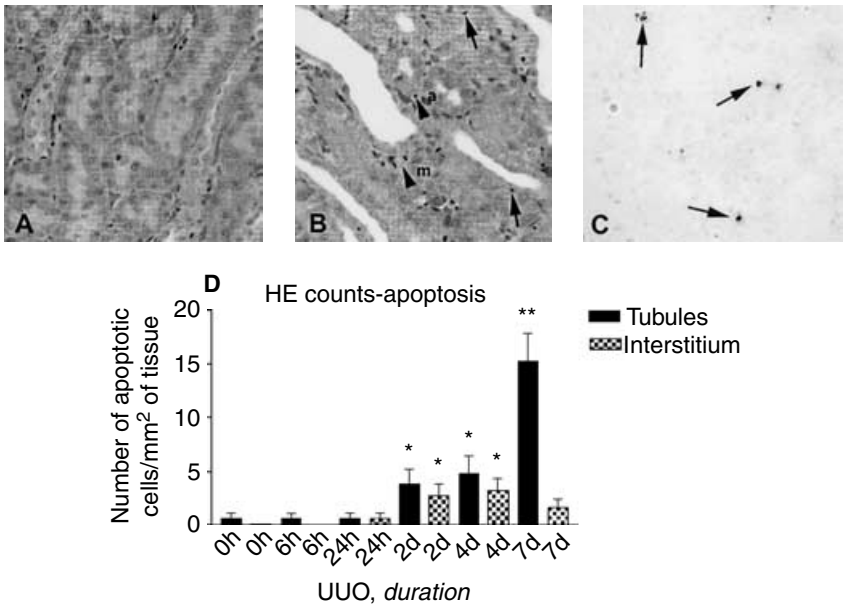

Fig. 6. Apoptosis in the tubulointerstitium. (*A* and *B*) Examples of hematoxylin and eosin–stained control (A) (no apoptosis) and 7 days' unilateral ureteral obstruction (UUO) kidney sections (B) (apoptosis in epithelium indicated with arrows and apoptosis in the interstitium indicated with arrowhead and letter "a; " mitosis in the interstitium indicated with arrowhead and letter "m"). (*C*) In situ end labeling (ISEL) verification of presence of apoptosis (examples of positive nuclei arrowed). Tubulointerstitial apoptosis increased from 2 days' UUO and peaked in the tubular epithelium at 7 days (*D*). $^{*}P < 0.05$; $^{**}P < 0.001$ compared with controls.

and increasing in UUO animals. Figure 7 shows a representative Western blot for pERK and ERK (total endogenous ERK) as well as the mean densitometry. There was a significant increase in pERK/ERK at 1 to 7 days UUO ($P < 0.05$). Localization of pERK was mainly in the collecting ducts of the inner medulla in controls (Fig. 8A), as part of a double stain with PCNA) and 6 hours' UUO animals. However, at later stages of UUO, pERK was

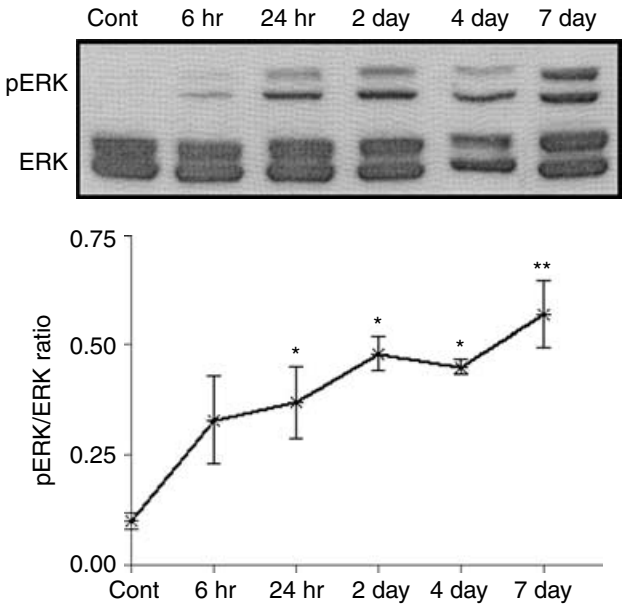

Fig. 7. Extracellular signal-regulated kinase (ERK) expression and activation. Western blot and densitometric analysis for phosphorylated ERK (pERK) and ERK (endogenous total ERK) are demonstrated. There was a significant increase in the levels of pERK/ERK at 24 hours to 7 days' unilateral ureteral obstruction (UUO) in comparison with controls. $^{*}P < 0.05$; $^{**}P < 0.01$.

seen in the outer medulla and cortex and was prevalent in tubular epithelial cells (Fig. 8B) (2 days' UUO), a result similar to that found by Masaki et al [38].

ERK activation and proliferation

Double labeling of pERK and PCNA in controls and 7 days' UUO animals is shown in Figure 8A and B. Figure 8C and D demonstrate the linear regression analysis of double-stained PCNA and pERK (pERK/PCNA) against pERK alone. The high R^2 values indicate a positive correlation ($P < 0.001$) between pERK expressing cells and PCNA, which strengthened with increasing duration of UUO (Fig. 8D), correlation coefficient.

ERK activation, apoptosis, and differentiation

Interstitial apoptotic cells had dual staining for pERK and Apoptag, however, the apoptotic cells in the tubular epithelium were rarely positive for pERK (Fig. 9A and B). Thus, there is some indication that pERK acts in the death pathway of interstitial cells, probably fibroblasts (see Fig. 2), but not the tubular epithelium. There were no dual-labeled cells for pERK and α-SMA in the interstitium or the tubular epithelium (Fig. 9C). Thus, pERK did not appear to act directly in the differentiation pathway of myofibroblasts. There were many pERK-positive epithelial cells adjacent to α-SMA–positive interstitial cells, indicating that there may be paracrine stimulation of these populations of cells. Figure 9D demonstrates pERK staining in human UUO tissue. There was spatial agreement of pERK localization between human and experimental samples, that is, there was labeling of the tubular epithelium but, rarely, interstitial cells.

Antioxidant modulation of fibrosis

Figure 10 demonstrates Western blot and densitometry for pERK, ERK, α-SMA, HO-1, and fibronectin, and also the 8-OHdG immunohistochemistry index, for control, 2 and 7 days' UUO animals, with and without antioxidant treatments (vitamin E, NAC, and fluvastatin). The controls for each antioxidant produced no changes significantly different from untreated controls and are not demonstrated. There was a significant increase in ERK activation in 2 days' UUO and UUO plus fluvastatin animals compared with controls ($P < 0.05$). ERK activation with fluvastatin was higher than the UUO levels ($P = 0.1243$). UUO alone and all UUO plus antioxidant treatments were associated with increased ERK activation at 7 days ($P < 0.05$), with NAC and fluvastatin associated with a significant decrease in pERK compared with UUO alone ($P < 0.05$). α-SMA was significantly increased in all UUO animals over controls ($P < 0.05$). Fluvastatin significantly decreased α-SMA compared with UUO alone at 2 days ($P < 0.05$). This was verified by immunohistochemistry (Fig. 11A and B controls) (Fig. 11C and D UUO alone) (Fig. 11E and F UUO plus fluvastatin). HO-1 expression was significantly increased in all UUO animals compared with controls. Although HO-1 expression did not decrease significantly at either 2 or 7 days with UUO cotreatments, the decrease neared significance at 7 days with fluvastatin ($P = 0.0821$). The 8-OHdG IHC index was significantly reduced at both 2 and 7 days with fluvastatin cotreatment compared with UUO alone ($P < 0.05$), verifying an antioxidant action. Both NAC and fluvastatin cotreatment significantly decreased fibronectin expression at 2 days and fluvastatin decreased fibronectin expression at 7 days ($P < 0.05$). Counts for apoptosis and mitosis are available in Figure 12. Results from controls and UUO alone are compared with the cotreatments plus UUO. Only fluvastatin induced a significant change from UUO alone, that being a reduction in tubular epithelial apoptosis at 7 days ($P < 0.05$).

DISCUSSION

Tubulointerstitial fibrosis is a common occurrence in many renal diseases, including ureteral obstruction by calculi or tumors, ischemia/reperfusion, and toxic nephropathies. It is often progressive and can be debilitating, leading to end-stage renal disease (ESRD). UUO is a well-established model of experimental renal injury that results in fibrosis of the tubulointerstitium via characteristic changes seen in human disease, such as expansion of the renal interstitium via excessive matrix proteins

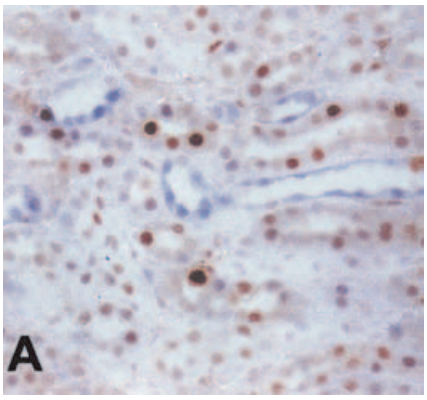

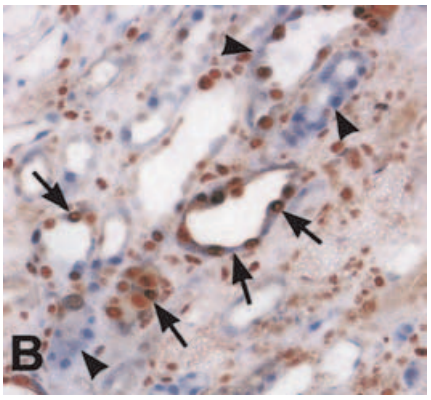

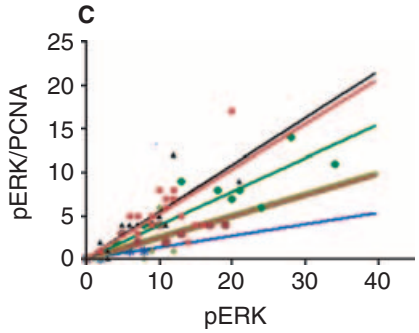

D

Animal group	R-squared	Correction coefficient (slope) in comparison to Control-no UUO (0hr)
6hr UUO	0.5707	0.064
24hr UUO	0.9337	0.127
2day UUO	0.9417	0.173
4day UUO	0.8595	0.355
7day UUO	0.8547	0.428

Fig. 8. Proliferating cell nuclear antigen (PCNA) and phosphorylated extracellular signal-regulated kinase (pERK) localization (double staining). (*A*) pERK/PCNA immunolocalization in control sections, where pERK was seen mainly in collecting ducts of the renal papilla and there were few double-labeled cells. (*B*) Localization in 2 days' unilateral ureteral obstruction (UUO) kidneys, where pERK was found in the tubular epithelium in the outer medulla and there were many dual-labeled epithelial cells. (*C*) The linear regression analysis for dual labeled pERK/PCNA cells against pERK-labeled cells. There was a significant correlation between the parameters ($P < 0.001$), with the correlation coefficient increasing with time (*D*).

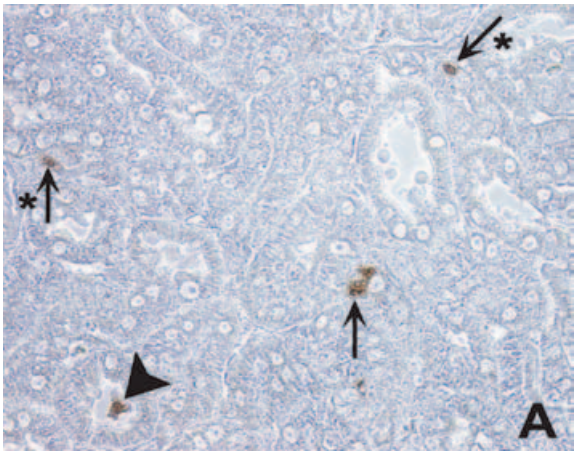

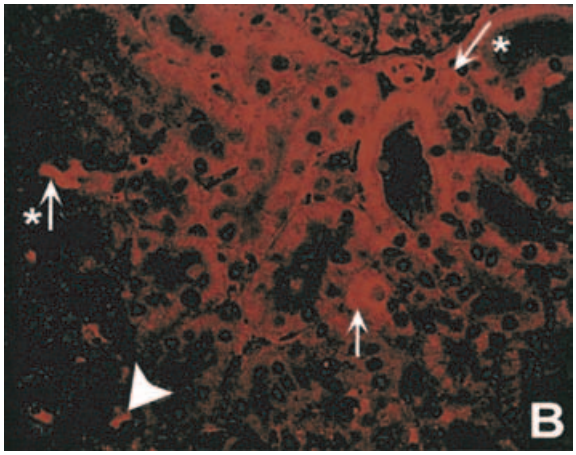

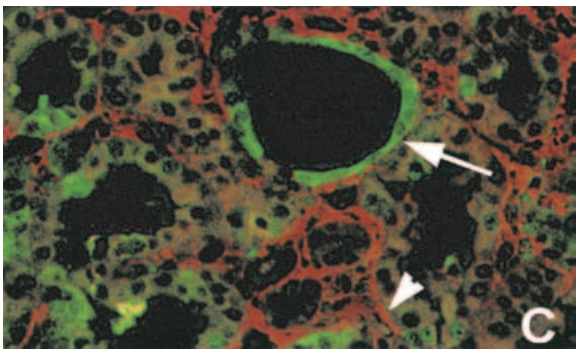

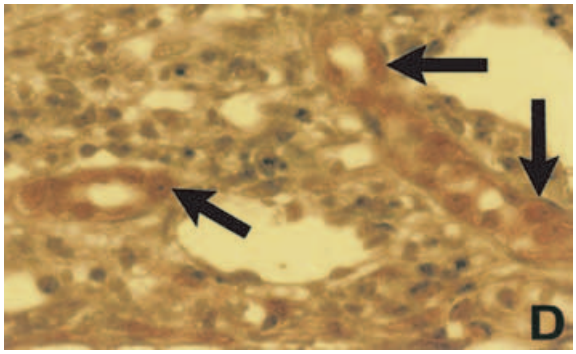

Fig. 9. Phosphorylated extracellular signal-regulated kinase (pERK) expression, apoptosis, and cell differentiation (double staining). (*A* and *B*) Dual labeling for apoptosis (brown nuclei) and pERK immunolocalization (red fluorescence) in 2 days' unilateral ureteral obstructed (UUO) kidneys. Apoptotic cells in the tubular epithelium (arrow with no asterisk) and the tubular lumen (arrowhead) did not have pERK coexpression. Interstitial apoptotic cells (arrows with asterisk) also expressed pERK. (*C*) Immunolocalization for pERK (green in tubular epithelium; arrow) and α-smooth muscle actin (α-SMA) (red in interstitial myofibroblasts; examples with arrowhead) is demonstrated in a 7 days' UUO kidney. There were no cells that stained positive for both proteins. (*D*) Human UUO tissue immunostained with pERK also demonstrated localization of the protein in the tubular epithelium (arrows), and not the interstitium.

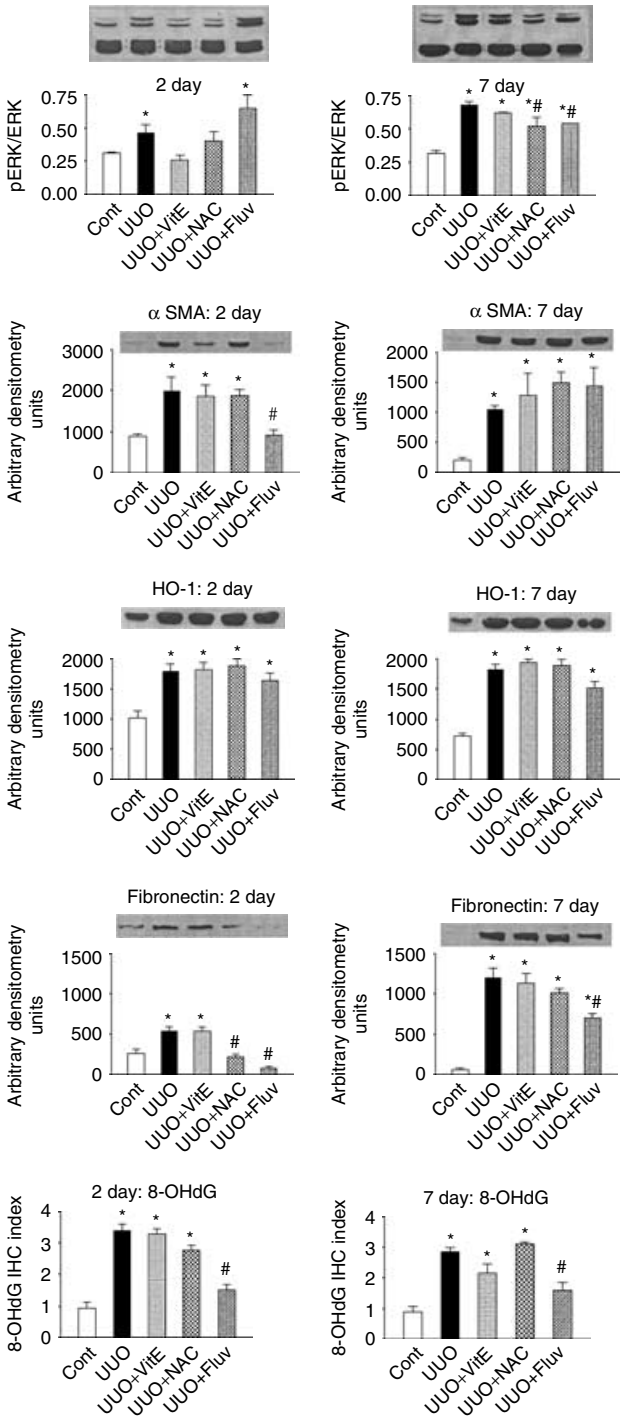

Fig. 10. Representative Western immunoblot and mean ± SEM of densitometry. Controls and 2 and 7 days' unilateral ureteral obstruction (UUO) animals with and without the antioxidants vitamin E (vit E), N-acetylcysteine (NAC), and fluvastatin (fluv), for extracellular signal-regulated kinase (ERK), phosphorylated ERK (pERK), α-smooth muscle actin (α-SMA), heme oxygenase-1 (HO-1), and fibronectin. The immunohistochemistry (IHC) index for 8-hydroxy-2′-deoxyguanosine (8-OHdG) is also demonstrated. $^*P < 0.05$ compared with controls; $\#P < 0.05$ compared with UUO alone.

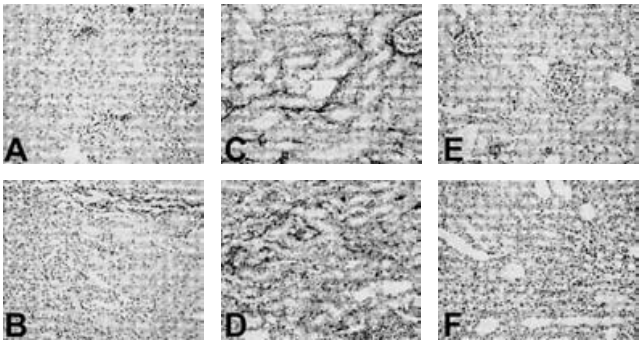

Fig. 11. Immunolocalization of α-smooth muscle actin (αSMA) is presented for controls and 2 days' unilateral ureteral obstruction (UUO) animals with and without fluvastatin. (*A*, *C*, and *E*) The cortex. (*B*, *D*, and *F*) The medulla. (A and B) Untreated controls. (C and D) UUO. (E and F) UUO plus fluvastatin. Expression of α-SMA in the fluvastatin-treated UUO animals is similar to baseline levels in untreated controls.

production, fibroblast activation or proliferation, monocyte and macrophage infiltration, and tubular atrophy. These changes may be mediated, in part, by intracellular pathways that are initiated by oxidative stress [18, 19, 39]. The present study verified the development of tubulointerstitial fibrosis by describing significant increases in ECM proteins and α-SMA–positive interstitial cells with increasing duration of UUO.

Oxidative stress plays a role in promoting renal fibrosis in some instances. Moriyama et al [12] recently demonstrated increased oxidative stress in the interstitium of UUO kidneys based on the increased expression of HO-1 mRNA and immunohistochemistry detection of advanced glycation end products (AGE) in the interstitium. AGE products can promote transdifferentiation of renal epithelial cells to a myofibroblast α-SMA–expressing phenotype [40]. Fluvastatin, a 3-hydroxy-3-methylglutaryl coenzyme A (HMG-CoA) reductase inhibitor, was used by Moriyama et al as antioxidant therapy in the UUO animals' diet and it caused a slight but significant attenuation of tubulointerstitial fibrosis, indicating a causal relationship between oxidative stress and renal fibrosis. Oxidative stress is difficult to measure directly in vivo, and the alternative of monitoring stress-inducible genes like HO-1 has found acceptance. HO-1 is the rate-limiting enzyme that catalyses heme degradation to bilverdin and ultimately to bilirubin, liberating carbon monoxide and free iron in the process [41]. Its induction occurs in cells and tissues after renal ischemia/reperfusion injury [42], hypertension [32], UUO [11, 12], and exposure to urea [43]. In addition, 8-OHdG is seen as a robust measure of oxidant-induced DNA damage [27]. The results of the present study verified an involvement of oxidative stress in UUO-induced fibrosis.

In progressive obstructive nephropathy, the renal tubules dilate and tubular epithelial cells undergo apoptosis, leading to tubular atrophy. There is also a high

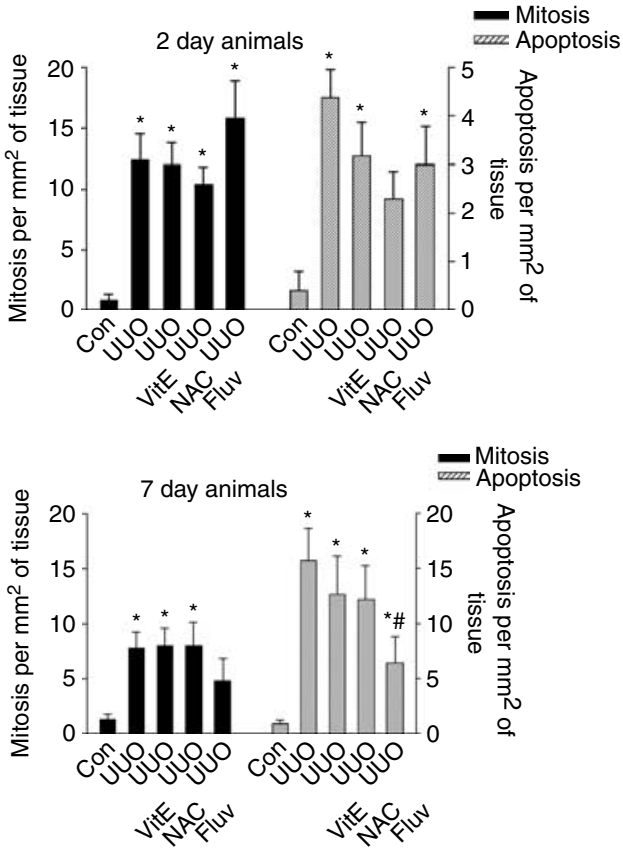

Fig. 12. The mean ± SEM of mitosis and apoptosis in the tubular epithelium is demonstrated for untreated controls, unilateral ureteral obstruction (UUO) and UUO plus antioxidants [vitamin E, N-acetylcysteine (NAC) and fluvastatin] at 2 and 7 days. In a comparison of UUO alone with UUO plus antioxidants, only fluvastatin (fluv) was associated with a significant decrease in tubular epithelial apoptosis. $^{*}P < 0.05$ compared with controls; $\#P < 0.05$ compared with UUO alone.

level of cell proliferation in the tubular epithelium in the early stages of fibrogenesis [6–8]. The present study confirmed these results and also established that moderate but significant interstitial cell proliferation and apoptosis occurred, demonstrating the dynamic nature of the interstitium during the development of fibrosis. The involvement of signal transduction pathways in this dynamic process of epithelial and interstitial cell proliferation and death has received little attention to date. The MAPK pathways are well characterized in other instances of cell proliferation and death [20, 44]. We had some indication, in renal fibrosis, that the pERK pathway had cell specific roles, promoting growth or protection of the renal tubular epithelium but cell death of renal fibroblasts after oxidative stress [19]. The present investigation sought to determine if this same association occurred in the in vivo UUO model of renal fibrosis, known to have similar causative features.

Western blot analysis indicated that pERK/ERK increased significantly at 1 to 7 days' UUO in comparison with controls, a result similar to that seen in renal tubular epithelial and fibroblast cells in vitro after oxidative stress. The positive relationship between pERK and promotion of epithelial cell growth and survival, seen in vitro after oxidative stress, was matched by the positive correlation between pERK and tubular epithelial proliferation (PCNA labeling) seen in vivo. Similar results have been published recently by others [38]. Dual labeling of pERK and apoptosis indicated that pERK did not act in the death pathway of tubular epithelial cells but there was some dual labeling of interstitial cells. pERK did not localize with α-SMA–expressing fibroblasts, indicating it does not act in their differentiation pathway in this in vivo model. A close spatial relationship between many pERK-positive epithelial cells and adjacent α-SMA–positive interstitial cells was seen, indicating that there may be paracrine stimulation of myofibroblasts, for example, by growth factors synthesized in the epithelium under the protective influence of pERK. A similar characteristic has been recorded previously where cortical fibroblasts benefited from paracrine stimulation by proximal tubular epithelial cells grown in vitro in close proximity to the fibroblasts [45].

There were few inconsistencies between the original in vitro model and this in vivo study, and these related mainly to the moderate levels of apoptosis seen in vivo versus the high levels that were able to be induced by oxidative stress in the in vitro model of renal fibrosis. A comparison of pERK expression and fibrosis from the models is summarized in Table 1. Differences between in vitro and in vivo results are not surprising, and similar disparities have been published elsewhere [46]. In the in vitro investigation that was used as a model for the present study [19], a single cause of fibrosis (oxidative stress) was analyzed against pERK activation in very specific renal cell populations (renal tubular epithelium, fibroblasts, and endothelium). The outcome mimicked some of the characteristics seen in renal fibrosis. We had been able to verify the cell-specific roles for pERK, in vitro, using the specific inhibitor (PD98059) of MEK (MAPK or ERK kinases), a precursor of ERK [19]. Undoubtedly, in vivo, the model is much more complex and the causes of fibrosis multifactorial. The ERK pathway is traditionally considered to act in cell proliferation and, sometimes, differentiation rather than cell death. The in vitro and now the in vivo UUO model also indicate a link between pERK and fibroblast or interstitial cell death.

The results of the present analysis of modulation of oxidative stress by antioxidants in UUO-induced fibrosis supported the work of Moriyama et al (2002) who reported an attenuation of tubulointerstitial fibrosis with fluvastatin treatment via an antioxidant mechanism. We have now demonstrated that this mechanism appears

Table 1. Summary of the spatiotemporal association between extracellular signal-regulated kinase (ERK) activation and fibrotic changes in the current in vivo model and the in vitro model [19] on which this study was based

	ERK activation in oxidant-associated fibrotic injury	
	Early	Late
In vitro [19]	Prevents early decrease in tubular epithelial survival	↑ ERK activity does not appear to affect long-term survival of tubular epithelial cells
In vivo	↑ ERK activity parallels increases in fibroblast apoptosis Association with tubular epithelial proliferation ↑ ERK activity may ↓ myofibroblast activation and fibronectin production via an antioxidant mechanism	Promotes fibroblast apoptosis ↑ ERK activity does not affect survival or apoptosis ↓ ERK activity may inhibit apoptosis and fibronectin production via an antioxidant mechanism Associated expression of pERK in apoptotic interstitial cells (possibly myofibroblasts) but not in viable cells

also to involve time-dependent changes in pERK, which may reduce the infiltration of myofibroblasts or excessive tubular apoptosis. Of the other antioxidants used in the present study, only NAC induced a significant decrease in fibronectin expression and tubular epithelial apoptosis. The present study also demonstrated, however, that there was a significant fluvastatin and NAC treatment-associated decrease in pERK compared with UUO alone at 7 days. In studies with rabbits, a reduction in cardiac fibrosis and hypertrophy with simvastatin treatment, a drug in the same statin class as fluvastatin, was also associated with a significant reduction in ERK activation [44]. The exact biologic outcome of the altered ERK activity still needs elucidation.

CONCLUSION

The present study has demonstrated a role for the activated ERK protein in renal fibrogenesis under the influence of oxidative stress. Expression of pERK in tubular epithelial cells was associated spatially and temporally with their proliferation. Interstitial fibroblasts expressed no pERK, except where they were apoptotic. Thus, the biologic outcome of altered pERK expression appears to be cell type–specific. Fluvastatin acted as an antioxidant and was the best of the three treatments analyzed in attenuating fibrosis. Fluvastatin also was associated with altered pERK, which continues to be an attractive antifibrotic signaling target. The antifibrotic benefit of modulation of one specific signal transduction pathway (Rho) has already been demonstrated by Nagatoya et al [47] in renal fibrosis. Thus, in a similar fashion, the value of modulated expression of pERK in promoting survival or proliferation of tubular epithelial cells but the death of fibroblasts needs further analysis.

ACKNOWLEDGMENTS

This research was supported by an International Postgraduate Research Scholarship from the University of Queensland to the first author and funding from Kidney Health Australia and a University of Queensland Research Development Grant. Cost of the color for figures 8 and 9 has been kindly paid for by a grant from Novartis Pharmaceuticals Australia Pty. Ltd.

Reprint requests to A/Professor Glenda Gobe, Department of Molecular and Cellular Pathology, School of Medicine, University of Queensland, Herston Road, Herston, Brisbane, Australia, 4006.
E-mail: g.gobe@uq.edu.au

REFERENCES

1. Hewitson TD, Kelynack KJ, Tait MG, *et al*: Pirfenidone reduces in vitro rat renal fibroblast activation and mitogenesis. *J Nephrol* 14:453–460, 2001
2. Sato N, Shiraiwa K, Kai K, *et al*: Mizoribine ameliorates the tubulointerstitial fibrosis of obstructive nephropathy. *Nephron* 89:177–185, 2001
3. Ng YY, Huang TP, Yang WC, *et al*: Tubular epithelial-myofibroblast transdifferentiation in progressive tubulointerstitial fibrosis in 5/6 nephrectomized rats. *Kidney Int* 54:864–876, 1998
4. Klahr S, Morrissey J: Obstructive nephropathy and renal fibrosis. *Am J Physiol Renal Physiol* 283:F861–F875, 2002
5. Gerth JH, Kriegsmann J, Trinh TT, *et al*: Induction of p27KIP1 after unilateral ureteral obstruction is independent of angiotensin II. *Kidney Int* 61:68–79, 2002
6. Gobe GC, Axelsen RA: Genesis of renal tubular atrophy in experimental hydronephrosis in the rat. Role of apoptosis. *Lab Invest* 56:273–281, 1987
7. Kennedy WA, Stenberg A, Lackgren G, *et al*: Renal tubular apoptosis after partial ureteral obstruction. *J Urol* 152:658–664, 1994
8. Zhang G, Oldroyd SD, Huang LH, *et al*: Role of apoptosis and Bcl-2/Bax in the development of tubulointerstitial fibrosis during experimental obstructive nephropathy. *Exp Nephrol* 9:71–80, 2001
9. Ricardo SD, Diamond JR: The role of macrophages and reactive oxygen species in experimental hydronephrosis. *Semin Nephrol* 18:612–621, 1998
10. Haugen E, Nath KA: The involvement of oxidative stress in the progression of renal injury. *Blood Purif* 17:58–65, 1999
11. Kawada N, Moriyama T, Ando A, *et al*: Increased oxidative stress in mouse kidneys with unilateral ureteral obstruction. *Kidney Int* 56:1004–1013, 1999
12. Moriyama T, Kawada N, Nagatoya K, *et al*: Fluvastatin suppresses oxidative stress and fibrosis in the interstitium of mouse kidneys with unilateral ureteral obstruction. *Kidney Int* 59:2095–2103, 2001
13. Nowzari FB, Davidson SD, Eshghi M, *et al*: Adverse effects of oxidative stress on renal cells and its prevention by antioxidants. *Mol Urol* 4:15–19, 2000
14. Schaaf GJ, Nijmeijer SM, Maas RF, *et al*: The role of oxidative stress in the ochratoxin A-mediated toxicity in proximal tubular cells. *Biochim Biophys Acta* 1588:149–158, 2002
15. Cuttle L, Zhang XJ, Endre ZH, *et al*: Bcl-X(L) translocation in renal tubular epithelial cells in vitro protects distal cells from oxidative stress. *Kidney Int* 59:1779–1788, 2001
16. Yuan B, Liang M, Yang Z, *et al*: Gene expression reveals vulnerability to oxidative stress and interstitial fibrosis of renal outer medulla to nonhypertensive elevations of ANG II. *Am J Physio Regul Integr Comp Physiol* 284:R1219–R1230, 2003

17. Cooper ME: Interaction of metabolic and haemodynamic factors in mediating experimental diabetic nephropathy. *Diabetologia* 44:1957–1972, 2001
18. Di Mari JF, Davis R, Safirstein RL: MAPK activation determines renal epithelial cell survival during oxidative injury. *Am J Physiol* 277:F195–F203, 1999
19. Pat B, Yang T, Watters D, *et al*: Fibrogenic stresses activate different mitogen-activated protein kinase pathways in renal epithelial, endothelial or fibroblast cell populations. *Nephrology* 8:192–200, 2003
20. Waskiewicz AJ, Cooper JA: Mitogen and stress response pathways: MAP kinase cascades and phosphatase regulation in mammals and yeast. *Curr Opin Cell Biol* 7:798–805, 1995
21. Force T, Bonventre JV: Growth factors and mitogen-activated protein kinases. *Hypertension* 31:152–161, 1998
22. Bokemeyer D, Guglielmi KE, McGinty A, *et al*: Activation of extracellular signal-regulated kinase in proliferative glomerulonephritis in rats. *J Clin Invest* 100:585–588, 1997
23. Wilmer WA, Tan LC, Dickerson JA, *et al*: Interleukin-1beta induction of mitogen-activated protein kinases in human mesangial cells: Role of oxidation. *J Biol Chem* 272:10877–10881, 1997
24. Xia Z, Dickens M, Raingeaud J, *et al*: Opposing effects of ERK and JNK-p38 MAP kinases on apoptosis. *Science* 270:1326–1331, 1995
25. Wang X, Martindale JL, Liu Y, *et al*: The cellular response to oxidative stress: Influences of mitogen-activated protein kinase signaling pathways on cell survival. *Biochem J* 333:291–300, 1998
26. Bhat NR, Zhang P: Hydrogen peroxide activation of multiple mitogen-activated protein kinases in an oligodendrocyte cell line: Role of extracellular signal-regulated kinase in hydrogen peroxide-induced cell death. *J Neurochem* 72:112–119, 1999
27. Mahmood S, Kawanaka M, Kamei A, *et al*: Immunohistochemical evaluation of oxidative stress markers in chronic hepatitis C. *Antioxid Redox Signal* 6:19–24, 2004
28. Ansari B, Coates PJ, Greenstein BD, *et al*: In situ end-labelling detects DNA strand breaks in apoptosis and other physiological and pathological states. *J Pathol* 170:1–8, 1993
29. Gobe G, Zhang X-J, Willgoss D, *et al*: Relationship between Bcl-2 genes, growth factors and apoptosis in acute ischemic renal injury in the rat. *J Am Soc Nephrol* 11:454–467, 2000
30. Kerr JF, Gobe GC, Winterford CM, *et al*: Anatomical methods in cell death. *Methods Cell Biol* 46:1–27, 1995
31. Vile GF, Tyrrell RM: Oxidative stress resulting from ultraviolet A irradiation of human skin fibroblasts leads to a heme oxygenase dependent increase in ferritin. *J Biol Chem* 268:14678–14681, 1993
32. Aizawa T, Ishizaka N, Taguchi J, *et al*: Heme oxygenase-1 is upregulated in the kidney of angiotensin II-Induced hypertensive rats: possible role in renoprotection. *Hypertension* 35:800–806, 2000
33. Nath KA, Grande JP, Haggard JJ, *et al*: Oxidative stress and induction of heme oxygenase-1 in the kidney in sickle cell disease. *Am J Pathol* 158:893–903, 2001
34. Akagi R, Takahashi T, Sassa S: Fundamental role of heme oxygenase in the protection against ischemic acute renal failure. *Jpn J Pharmacol* 88:127–132, 2002
35. Shibahara S, Muller R, Taguchi H, *et al*: Cloning and expression of cDNA for rat heme oxygenase. *Proc Natl Acad Sci USA* 82:7865–7869, 1985
36. Klahr S, Harris K, Purkerson ML: Effects of obstruction on renal functions. *Pediatr Nephrol* 2:34–42, 1988
37. Lane A, Johnson DW, Pat B, *et al*: Interaction roles of myofibroblasts, apoptosis and fibrogenic growth factors in the pathogenesis of renal tubulointerstitial fibrosis. *Growth Factors* 20:109–119, 2002
38. Masaki T, Foti R, Hill PA, *et al*: Activation of the ERK pathway precedes tubular proliferation in the obstructed rat kidney. *Kidney Int* 63:1256–1264, 2003
39. Eddy AA: Molecular basis of renal fibrosis. *Pediatr Nephrol* 15:290–301, 2000
40. Oldfield MD, Bach LA, Forbes JM, *et al*: Advanced glycation end products cause epithelial-myofibroblast transdifferentiation via the receptor for advanced glycation end products (RAGE). *J Clin Invest* 108:1853–1863, 2001
41. Maines MD: Heme oxygenase: function, multiplicity, regulatory mechanisms, and clinical applications. *FASEB J* 2:2557–2568, 1988
42. Horikawa S, Yoneya R, Nagashima Y, *et al*: Prior induction of heme oxygenase-1 with glutathione depletor ameliorates the renal ischemia and reperfusion injury in the rat. *FEBS Lett* 510:221–224, 2002
43. Tian W, Bonkovsky HL, Shibahara S, *et al*: Urea and hypertonicity increase expression of heme oxygenase-1 in murine renal medullary cells. *Am J Physiol Renal Physiol* 281:F983–F991, 2001
44. Tibbles LA, Woodgett JR: The stress-activated protein kinase pathways. *Cell Mol Life Sci* 55:1230–1254, 1999
45. Johnson DW, Saunders HJ, Baxter RC, *et al*: Paracrine stimulation of human renal fibroblasts by proximal tubule cells. *Kidney Int* 54:747–757, 1994
46. Shao R, Tarloff JB: Lack of correlation between para-aminophenol toxicity in vivo and in vitro in female Sprague-Dawley rats. *Fundam Appl Toxicol* 31:268–278, 1996
47. Nagatoya K, Moriyama T, Kawada N, *et al*: Y-27632 prevents tubulointerstitial fibrosis in mouse kidneys with unilateral ureteral obstruction. *Kidney Int* 61:1684–1695, 2002